Published in final edited form as:
Pulm Pharmacol Ther. 2013 April ; 26(2): . doi:10.1016/j.pupt.2012.12.004.

Chronic Inhibition of PPAR-γ Signaling Induces Endothelial Dysfunction In The Juvenile Lamb

Shruti Sharma[1], **Jubilee Barton**[2], **Ruslan Rafikov**[1], **Saurabh Aggarwal**[1], **Hsuan-Chang Kuo**[2], **Peter E. Oishi**[2,3], **Sanjeev A. Datar**[2], **Jeffrey R Fineman**[2,3], and **Stephen M. Black**[1]

[1]Vascular Biology Center, Georgia Health Sciences University, Augusta, GA 30912

[2]Department of Pediatrics, University of California, San Francisco, San Francisco, CA, 94143

[3]Cardiovascular Research Institute, University of California, San Francisco, San Francisco, CA, 94143

Abstract

We have recently shown that the development of endothelial dysfunction in lambs with increased pulmonary blood flow (PBF) correlates with a decrease in peroxisome proliferator activated receptor-γ (PPAR-γ) signaling. Thus, in this study we determined if the loss of PPAR-γ signaling is necessary and sufficient to induce endothelial dysfunction by exposing lambs with normal PBF to the PPAR-γ antagonist, GW9662. Two-weeks of exposure to GW9662 significantly decreased both PPAR-γ protein and activity. In addition, although eNOS protein and nitric oxide metabolites (NO_x) were significantly increased, endothelial dependent pulmonary vasodilation in response to acetylcholine was attenuated, indicative of endothelial dysfunction. To elucidate whether downstream mediators of vasodilation were impaired we examined soluble guanylate cyclase (sGC)- α and β subunit protein, cGMP levels, and phosphodiesterase 5 (PDE5) protein and activity, but we found no significant changes. However, we found that peroxynitrite levels were significantly increased in GW9662-treated lambs and this correlated with a significant increase in protein kinase G-1α (PKG-1α) nitration and a reduction in PKG activity. Peroxynitrite is formed by the interaction of NO with superoxide and we found that there was a significant increase in superoxide generation in GW9662-treated lambs. Further, we identified dysfunctional mitochondria as the primary source of the increased superoxide. Finally, we found that the mitochondrial dysfunction was due to a disruption in carnitine metabolism. We conclude that loss of PPAR-γ signaling is sufficient to induce endothelial dysfunction confirming its important role in maintaining a healthy vasculature.

Keywords

mitochondrial dysfunction; NO signaling; carnitine metabolism; oxidative stress

INTRODUCTION

Multiple lines of evidence indicate that the increased pulmonary blood flow (PBF) associated with various congenital heart defects results in endothelial injury and the development of pulmonary vascular disease. Indeed, early endothelial dysfunction, as displayed by histologic endothelial abnormalities, impairment of endothelium-dependent pulmonary vasodilation, and increased ET-1 levels, has been described in children with

Please address correspondence and proofs to: Stephen M. Black, PhD, Vascular Biology Center, 1459 Laney Walker Blvd, CB3210B, Georgia Health Sciences University, Augusta, GA 30912, sblack@georgiahealth.edu.

congenital heart defects and pulmonary hypertension [1–3]. The precise mechanisms linking increased pulmonary blood flow to this endothelial dysfunction are incompletely understood. Utilizing our ovine model of a congenital heart defect with increased pulmonary blood flow, we have demonstrated similar evidence of endothelial dysfunction, including impaired endothelium-dependent pulmonary vasodilation, increased pulmonary vascular reactivity, altered NO-cGMP signaling, and increased superoxide levels. Our recent data have shown that the development of endothelial dysfunction in lambs with increased PBF correlates with a decrease in peroxisome proliferator-activated receptor-γ (PPAR-γ) expression [4].

Peroxisome proliferator-activated receptors (PPARs) are a group of nuclear receptor proteins that function as transcription factors by regulating the expression of genes. Altered PPAR signaling has been shown to be involved in the development of both systemic and pulmonary vascular disease [5]. PPAR-γ in particular, has been implicated in the pathology of several diseases including obesity, diabetes, atherosclerosis, and cancer [6, 7]. Earlier studies in endothelial cells (EC) have shown that PPAR-γ is an important regulator of hypertension [8] and disruption of PPAR-γ signaling in EC is sufficient to cause PAH [9]. Other studies have also shown the potential role for PPAR-γ signaling in the progression of pulmonary hypertension disease in adults [10, 11] and children [4]. However, the role of PPAR-γ signaling in mediating early endothelial dysfunction has not been investigated.

Thus, in this study we wanted to determine if the early loss of PPAR-γ signaling in lambs with increased PBF [4] is causally related to the development of endothelial dysfunction. To accomplish this we exposed newborn lambs with normal PBF to the PPAR-γ antagonist, GW9662 for two weeks. Our data indicate that although NO levels are increased in GW9662-treated lambs there is endothelial dysfunction secondary to a nitration-mediated inhibition of PKG-1α. Our data also indicate that the increase in peroxynitrite is mediated by increased superoxide generation from the mitochondria. Finally, we found that the mitochondrial dysfunction induced by GW9662 treatment is due to a disruption of carnitine homeostasis. Thus, we conclude that loss of PPAR-γ signaling alone is sufficient to induce pulmonary endothelial dysfunction.

MATERIALS & METHODS

Exposure of lambs to GW9662

Within 24 hours of spontaneous delivery, normal lambs received single daily intravenous (IV) injections of the PPAR-γ antagonist-GW9662 (1mg/kg/day) or vehicle (DMSO, 0.03 ml/kg/day) for two weeks. At two weeks of age, the lambs were anesthetized with ketamine hydrochloride (15 mg/kg IM). Polyurethane catheters were placed in an artery and vein of a hind leg and advanced to the descending aorta and the inferior vena cava, respectively. The lambs were then anesthetized with ketamine hydrochloride (~0.3 mg/kg/min), diazepam (0.002 mg/kg/min), and fentanyl citrate (1.0 μg/kg/hr), intubated with a 7.0 mm OD cuffed endotracheal tube, and mechanically ventilated with a V.I.P Bird® Sterling (Palm Springs, CA) time-cycled, pressure-limited ventilator. Mechanical ventilation was adjusted to maintain pCO_2 between 35 and 40 mmHg and pH between 7.35 and 7.40. Hemoglobin was maintained above 7 g/dL, using fresh whole blood transfusions from the ewe as required. Sodium bicarbonate was administered to correct metabolic acidosis if it occurred. The inspired oxygen concentration was maintained at 21%. The lambs were maintained normothermic (39°C) with a heating blanket. With strict aseptic technique, a midsternotomy incision was then performed. Using a purse-string suture technique, polyurethane catheters were placed directly into the right and left atrium, and main pulmonary artery. An ultrasonic flow probe (Transonics Systems, Ithaca, NY) was placed around the left pulmonary artery to measure pulmonary blood flow. Following a 60 minute recovery period, baseline

hemodynamic variables and blood flows were recorded. A peripheral lung biopsy was then obtained for analysis, and vascular reactivity was determined (see below).

At the end of the protocol, all lambs were killed with a lethal injection of sodium pentobarbital followed by bilateral thoracotomy as described in the NIH Guidelines for the Care and Use of Laboratory Animals. All protocols and procedures were approved by the Committee on Animal Research of the University of California, San Francisco and the Georgia Health Sciences University, Augusta, Georgia.

Pulmonary vascular reactivity measurements

Following a 30 minute recovery, acetylcholine (Ach) chloride (1μg/kg) followed by inhaled NO (40 ppm) were administered. Ach chloride (IOLAB, Claremont, CA) was diluted in sterile 0.9% saline and delivered by rapid injection into the pulmonary artery. Inhaled NO was delivered to the inspiratory limb of the respiratory circuit (Inovent, Ohmeda Inc., Liberty, N.J.), and continued for 15 minutes. The inspired concentrations of NO and nitrogen dioxide were continuously quantified by electrochemical methodology (Inovent, Ohmeda Inc., Liberty, N.J.). The hemodynamic variables were monitored and recorded continuously. A minimum of 30 minutes separated the administration of ACh and inhaled NO, and the second agent was not given until baseline hemodynamics returned.

PPAR- γ transcriptional activity assay

The PPAR-γ Transcription Factor Assay kit (Cayman Chemical Company, Ann Arbor, MI) was used according to the manufacturer's protocol.

Western blot analysis

Protein extracts from peripheral lung tissue were prepared using lysis buffer (50mM Tris-HCl, pH 7.6, 0.5%Triton X-100, 20% glycerol) containing Halt™ protease inhibitor cocktail (Pierce Laboratories, Rockford, IL). The extracts were then subjected to centrifugation (15,000 g × 15min at 4°C). Supernatant fractions were assayed for protein concentration using the Bradford reagent (Bio-Rad, Richmond, CA) and used for Western blot analyses. Protein extracts (25–50μg) were separated on Long-Life 4–20% Tris-SDS-Hepes gels (Frenchs Forest, Australia) and electrophoretically transferred to Immuno-Blot™ PVDF membrane (Bio-Rad Laboratories, Hercules, CA). The membranes were blocked with 5% nonfat dry milk in Tris-buffered saline containing 0.1% Tween 20 (TBST). After blocking, the membranes were probed with antibodies to PPAR-γ, CrAT, sGC-α1, sGC-β1, PKG-1α (Santa Cruz Biotechnology, Inc.), CPT1, CPT2 (Affinity Bioreagents), eNOS (BD Transduction Laboratories), or PDE5 (Sigma). Reactive bands were visualized using chemiluminescence (SuperSignal® West Femto Substrate Kit, Pierce Laboratories, Rockford, IL) on a Kodak 440CF image station (Kodak, Rochester, NY). Band intensity was quantified using Kodak 1D image processing software. Expression of each protein was normalized by reprobing with β-actin used as an equal loading control (Sigma, St. Louis, MO).

Measurement of carnitine homeostasis

Detection of carnitines was performed using a Shimadzu UFLC system with a 5μm Omnispher C18 column (250 × 4.6mm OD) and equipped with an RF-10AXL fluorescence detector (Shimadzu USA Manufacturing Corporation). Total and free carnitine levels were quantified by fluorescence detection at 248 nm (excitation) and 418 nm (emission). Acyl carnitines were calculated as total carnitine minus free carnitine as previously published [12].

Measurement of peroxynitrite levels

The formation of peroxynitrite was determined by the peroxynitrite dependent oxidation of dihydrorhodamine (DHR) 123 to rhodamine 123, as described previously [13]. The tissue was pulverized; 10mg of tissue was placed in a microfuge tube, 100μl of 1xPBS was added, and the tissue was vortexed 3x for 10sec. The lysate was incubated with PEG-Catalase (100U) for 30min and then added to a 96 well black plate in the presence of 5μmol/L DHR 123 in 1xPBS for 1h. In both cases, the fluorescence of rhodamine 123 was measured at excitation 485nm and emission 545nm using a Fluoroskan Ascent Microplate Fluorometer.

Measurement of nitrated proteins

The total nitrated protein levels were measured in the lung homogenates. Briefly, 30μg protein was applied to a nitrocellulose membrane pre-soaked with Tris-buffered saline (TBS). After the protein samples were completely transferred, the membrane was blocked in 5% fat-free milk for 1h, washed with TBS, and incubated with mouse anti-3-nitrotyrosine (1:100, Calbiochem) antibody overnight. Finally, the membrane was incubated with goat anti-mouse IgG for 2h. The reactive dots were visualized using chemiluminescence (Pierce Laboratories) on a Kodak 440CF image station (New Haven, CT). The band intensity was quantified using Kodak 1D image processing software. The protein expression was normalized by re-probing with mouse anti β-actin antibody.

Immunoprecipitation analysis

Peripheral lung tissue were homogenized in 3x weight/volume of IP buffer (25mM Hepes, pH 7.5, 150mM NaCl, 1% NP-40, 10mM $MgCl_2$, 1mM EDTA, 2% glycerol, supplemented with protease inhibitor). Homogenates were then centrifuged at 20,000g at 4°C for 10min, the tissue supernatant was collected, and protein concentration was determined. To 1000μg of total protein, 4μg of antibody against PKG-1α or Hsp90 were added; the volume was brought to 1ml with IP buffer, and the mixture was nutated at 4°C overnight. To precipitate the bound protein, 30μl of protein G plus agarose suspension (EMD biosciences, Inc., San Diego, CA) was added, and the samples were nutated for 2h at 4°C. To collect the bead-bound antibody, the samples were then centrifuged at 2000g for 5min, the supernatant was removed, and the beads were washed 3x with 500μl of IP buffer. To the samples, 30μl of 2x Laemmli buffer was added, and the samples were boiled for 5min and then resolved using 4–20% Tris-SDS-Hepes PAGE. The membrane was then probed for 3-nitrotyrosine (1:100 dilution) or eNOS (1:1000), as described above. IP efficiency was normalized by re-probing with PKG-1α or Hsp90.

Determination of PKG activity

Total PKG activity was determined using a non-radioactive immunoassay to measure PKG mediated phosphorylation of a synthetic substrate, according to the manufacturer's directions. 8-Br cGMP was used to activate PKG to ensure that endogenous cGMP was not a limiting factor. The results were reported as pmols of phosphate incorporated into the GST-G substrate fusion protein in the presence of cGMP (10μM) per minute at 30°C per μg of PKG protein (pmol/min/μg).

Measurement of cGMP levels

cGMP levels in peripheral lung tissue were measured using an immunoassay based EIA kit (Cayman Chemicals, Ann Arbor, Michigan), according to the manufacturer's protocol.

Measurement of phosphodiesterase 5 activity

For determination of PDE5 activity, peripheral lung protein extracts (~25 μg) were incubated in the presence of DMSO or the PDE5 inhibitor, sildenafil (1 μM), for 1 h at room

temperature in a 1.5 ml microfuge tube. The levels of cGMP were measured using an immunoassay based EIA kit, according to the manufacturer's protocol. The difference between cGMP levels in samples in the presence and absence of sildenafil was presumed to be the cGMP degraded by PDE5, and therefore, a measurement of PDE5 activity. Results are reported as fmols of cGMP degraded per minute at 25°C per μg of total protein (fmol/min/μg).

Measurement of superoxide levels in lung tissue

To detect superoxide generation in lung tissue, we performed electron paramagnetic resonance (EPR) measurements. Fresh frozen tissues were pulverized in liquid nitrogen temperature (−196C) to form fine tissue powder. 4–6 mg of tissue powder was dissolved in 300μL of EPR buffer (PBS supplemented with 5 μM diethyldithiocarbamate and 25μM desferrioxamine; Sigma-Aldrich) at 0°C in temperature controlled cooling shaker (UltraCruz; Santa Cruz). This generates tissue particle suspension with intact, not lysed cells. We found that at 0°C tissue suspension does not generate measurable amount of superoxide. Dissolved powder was separated (75μL) between four 1.5 ml tubes containing spin probe CMH (5mg/ml) only, CMH and NOS inhibitor ETU(1mM), CMH and superoxide scavenger DHE (5μM), CMH and NADPH inhibitor Apocynin (10μM), CMH and XO inhibitor Allopurinol (1mM), CMH and mitochondria respiratory chain inhibitor Rotenone (1mM); and incubated for 2 min at 0°C. We utilized DHE to scavenge superoxide instead of PEG-SOD due to higher cell permeability for DHE. Doses of PEG-SOD up to 200U did not scavenge superoxide as efficiently as 5μM DHE. 30μl of tissue suspension from each tube was transferred to the glass capillary at room temperature to start enzymatic superoxide generation. Generation of superoxide in capillary took place for 30 min at room temperature. Superoxide radical generation was measured by reaction with spin probe CMH at room temperature in Magnettech M100 instrument (Magnettech, Germany). EPR spectra were analyzed for amplitude using ANALYSIS 2.0 software (Magnettech). To quantitate the amount of superoxide per milligram of protein, we also performed a standard reaction of the superoxide-generating enzyme xanthine oxidase in the presence of xanthine and CMH. A reaction curve was generated by adding 1mU of xanthine oxidase in the presence of xanthine ((Sigma) 1mM in PBS, pH 7.4, in the EPR reaction buffer and CMH) with 1nM/min superoxide generation rate over 1hour at room temperature. Final superoxide generation rate was expressed as pmol/min/mg of tissue.

Measurement of NO_x levels in lung tissue

Samples were deproteinized by adding cold ethanol (1:4; v/v). 0.05g of potassium iodide (KI) was dissolved in 7ml of freshly prepared acetic acid (AA). The KI/AA reagent was then added to a septum sealed purge vessel and bubbled with nitrogen gas. The gas stream was connected via a trap containing 1N NaOH to a Sievers 280i Nitric Oxide Analyzer (GE). Deproteinized samples were injected with a syringe through a silicone/Teflon septum. Results were analyzed by measuring the area under curve of the chemiluminescence signal using the Liquid software (GE).

Statistical analyses

This was performed using GraphPad Prism version 4.01 for Windows (GraphPad Software, San Diego, CA). The mean ± SEM or SD were calculated for all samples and significance was determined by the unpaired t-test. A value of $p<0.05$ was considered significant.

RESULTS

PPAR-γ inhibition significantly decreases PPAR-γ expression and activity in the juvenile lamb lung

At birth, lambs were exposed to either the vehicle (DMSO) or the PPAR-γ antagonist GW9662 (1mg/kg/day) for two weeks. At the end of the exposure period we examined the effect of PPAR-γ inhibition on PPAR-γ protein levels and activity. Our data indicate that there was a significant (>50%) reduction in PPAR-γ protein levels in GW9662-treated lambs (Figure 1 A). PPAR-γ DNA binding activity was also significantly decreased in GW9662-treated lambs (Figure 1 B).

PPAR-γ inhibition significantly increases eNOS expression and NO_x levels in the juvenile lamb lung

We have previously demonstrated that the loss of PPAR-γ signaling in lambs with increased PBF [14] correlates with an increase in eNOS protein levels but a reduction in NO signaling [15]. Our data indicate that similar to lambs with increased PBF, GW9662 treatment increased eNOS protein levels (Figure 2 A). However, unlike lambs with increased PBF, we found that NO_x levels are also increased in GW9662-treated lambs (Figure 2 B).

PPAR-γ inhibition leads to pulmonary endothelial dysfunction in the juvenile lamb

We have previously demonstrated that the loss of PPAR-γ signaling in lambs with increased PBF [14] correlates with a selective impairment in pulmonary vascular endothelium-dependent relaxation [16]. In the current study we found that GW9662 treatment did not alter baseline hemodynamics (Table 1). However, GW9662 treatment significantly attenuated the endothelium-dependent vasodilator Ach chloride (1μg/kg) did not decrease pulmonary arterial pressure (PAP, Figure 3 A) or pulmonary vascular resistance (PVR, Figure 3 B) in GW9662-treated lambs despite the apparent increase in NO signaling (Figure 2).

PPAR-γ inhibition does not alter cGMP signaling in the juvenile lamb lung

NO induces vasodilation through its ability to stimulate sGC activity to increase cGMP levels [17]. Cyclic GMP levels are in turn reduced by the activity of PDE5 [18]. Thus, we next determined if the endothelial dysfunction associated with GW9662-treatment was associated with a disruption in the ability of the lambs to generate cGMP or an increase in its degradation. However, our data indicate that there were no changes in the protein levels of sGC-α1 (Figure 4 A), sGC-β1 (Figure 4 B) or PDE5 (Figure 4 C). Similarly, we could find no changes in either PDE5 activity (Figure 4 D) or cGMP levels (Figure 4 E) between DMSO- or GW9662-treated lambs.

PPAR-γ inhibition attenuates PKG-1α activity in the juvenile lamb lung

We have recently identified a novel mechanism through which NO signaling can be disrupted. This is the nitration-mediated inhibition of PKG-1α [13]. To determine if this was occurring in GW9662-treated lambs we first determined the levels of peroxynitrite. Using both the oxidation of DHR123 (Figure 5 A) and dot blot analysis to measure total nitrated proteins (Figure 5 B), we found that peroxynitrite levels were significantly higher in GW9662-treated lambs. Further, our data indicate that the increase in peroxynitrite levels, leads to increased PKG-1α nitration (Figure 6 A) and decreased PKG activity (Figure 6 B) in the GW9662-treated lambs.

PPAR-γ inhibition increases mitochondrial superoxide generation in the juvenile lamb lung

Peroxynitrite is generated by the interaction of NO with superoxide. Thus, we next determined if superoxide levels were increased in GW9662-treated lambs. Our EPR data indicate that total superoxide levels were increased in GW9662- treated lambs (Figure 7). Further, we found no changes in NADPH oxidase derived superoxide (Figure 7). We also identified a modest, but significant, increase in NOS-derived superoxide (Figure 7). However, the majority of the increased superoxide appeared to be mitochondrial derived (Figure 7), suggesting that GW9662-the PPAR-γ antagonist, is causing mitochondrial dysfunction.

PPAR-γ inhibition disrupts Hsp90/eNOS interactions and carnitine homeostasis in the juvenile lamb lung

The interaction of the molecular chaperone, Hsp90 with eNOS has been shown to increase eNOS coupling [19]. Thus, we next determined if a reduction in the interaction of eNOS with hsp90 could underlie the increase in eNOS derived superoxide (Figure 7). Using immunoprecipitation analyses we found that GW9662 treated lambs had significantly less binding of Hsp90 to eNOS compared to DMSO-treated control lambs (Figure 8).

We have previously shown that there is a correlation between a loss of PPAR-γ signaling, mitochondrial dysfunction and the disruption of carnitine homeostasis in lambs with increased PBF [4]. Thus, we determined whether GW9662 was disrupting carnitine homeostasis. Compared to DMSO-treated control lambs, carnitine palmitoyltransferase 1 (CPT1, Figure 9 A), carnitine palmitoyltransferase 2 (CPT2, Figure 9 B) and carnitine acetyl transferase (CrAT, Figure 9 C) protein levels were reduced in GW9662-treated lambs. The decreases in the carnitine biosynthetic enzymes correlated with an increase in both acyl-carnitine (Figure 9 D) and the acyl-carnitine (AC) to free carnitine (FC) ratio (Figure 9 E) in GW9662-treated lambs indicating that carnitine homeostasis is disrupted.

DISCUSSION

Peroxisome proliferator-activated receptors (PPARs) are ligand-activated transcription factors belonging to the nuclear hormone receptor superfamily, that includes receptors for steroid hormones, thyroid hormones, retinoic acid, and fat-soluble vitamins [20]. Since their discovery over three decades ago it has become apparent that PPARs play a role in a number of processes, including lipid and glucose metabolism, diabetes and obesity, atherosclerosis, cellular proliferation and differentiation, neurological diseases, and inflammation and immunity [6, 21, 22]. Data from both our labs, and others, have begun to elucidate the important role played by PPAR-γ signaling in the pathogenesis of pulmonary hypertension. We have recently shown that lung PPAR-γ protein levels are reduced in our ovine model of pulmonary hypertension secondary to increased PBF [4]. Further, we have found that the PPAR-γ agonist, rosiglitazone, prevents the loss of NO signaling in our lamb model with increased PBF [23]. A similar protective effect has been observed in the mouse, where activating PPAR-γ with rosiglitazone reduced the development of hypoxia-induced pulmonary hypertension [24, 25]. Studies in humans have also identified a reduction in PPAR-γ mRNA [26] and protein in lungs from patients with advanced pulmonary hypertension [10]. However, the development of the endothelial dysfunction and the increase in vascular remodeling observed during the development of pulmonary hypertension is complex. This is especially true in our lamb model with increased PBF in which, beginning immediately after birth, the pulmonary vasculature is subjected to pathologic mechanical forces, including chronically increased shear stress. Thus, it is difficult to identify causal signaling nodes that are important for the development of endothelial dysfunction and the subsequent vascular remodeling associated with pulmonary

hypertension. The data we present here is thus important as it is the first study in the neonate that demonstrates that the attenuation of PPAR-γ alone is sufficient to induce endothelial dysfunction. Further, the mechanism by which this occurs, likely involves the nitration-mediated inhibition of PKG-1α and which we have also observed in our lambs with increased PBF [13]. Our identification of PKG inhibition via nitration in GW9662-treated lambs is an important finding as it adds to the increasing literature that shows that PKG-1α is sensitive to regulation by oxidative and nitrosative stress. We have recently demonstrated that the activity of recombinant PKG-1α is attenuated by exposure NO and hydrogen peroxide(H_2O_2), but not by superoxide [27]. However, there is conflicting data on the effect of H_2O_2 on PKG as a recent study has shown that it can also activate PKG-1α [28]. Further, in recent published studies we, and others, have identified a nitration dependent impairment of PKG-Iα activity in lambs with rebound pulmonary hypertension [13], increased pulmonary blood flow [13], in patients idiopathic pulmonary arterial hypertension [29], and in recombinant PKG-Iα exposed to authentic peroxynitrite [27]. Nitration of Y345 and Y549 in PKG-Iα has been linked to its inhibition [29]. This is based on a protein wide mutation analysis where all tyrosine residues in the catalytic domain of human PKG-Iα were mutated into phenylalanine [29]. However, these data must be interpreted cautiously as mass spectroscopy analyses were not carried out to confirm that Y345 and Y549 as the actual nitration sites. In addition, it is still unexplained how nitration results in the inhibition of PKG-Iα.

It is also worth noting differences we have observed between the normal lambs-treated with GW9662 and our lambs with increased PBF. Lambs with increased PBF have increased levels of cGMP, unlike the GW9662-treated lambs. This increase is mediated via stimulation of particulate guanylate cyclase activity by BNP [30] and despite increased PDE5 activity [31]. We did not find changes in PDE5 activity with GW9662-treatment alone. In addition, lambs with increased PBF also exhibit increases in superoxide generation from NADPH oxidase [32, 33] and xanthine oxidase [33]. However, we did not observe this in the GW9662-exposed lambs. It is unclear why PPAR-γ inhibition alone is insufficient to mimic all the effects of increased PBF but it is likely that there are other pathways dysregulated by the aberrant biomechanical forces that are not regulated by PPAR-γ inhibition. Indeed our microarray data demonstrate that the gene expression changes induced by PPAR-γ inhibition, although similar to those obtained in lambs with increased PBF, is not identical [14, 34]. Alternatively, it is possible that, similar to the lambs with increased PBF, there are dynamic changes that are occurring in the GW9662-exposed lambs. For example, our published data indicate that NADPH oxidase-and xanthine oxidase-dependent superoxide generation is increased at 2- and 4-, but not 8-weeks of age in lambs with increased PBF [33] while at one week of age, pulmonary vascular reactivity and endothelium-dependent pulmonary vasodilation are intact, with normal eNOS protein and mRNA levels and activity [35]. However, there is an age-dependent decline in NO signaling in lambs with increased PBF that correlates with a progressive increase in eNOS uncoupling [36]. Interestingly, although NO_x levels were significantly increased in GW9662-treated lambs we also found that NOS-derived superoxide, a measure of NOS uncoupling, was also significantly increased. This uncoupling was associated with a reduction in the interaction of eNOS with Hsp90. Hsp90 is known to play an important role in maintaining eNOS in a coupled state although the mechanism by which this occurs remains unclear [37]. We have also observed reduced eNOS-Hsp90 interactions in our lambs with increased PBF [36]. Indeed, there is a progressive developmental decline in eNOS-Hsp90 interactions in these lambs [36]. Again suggesting that there could be progressive changes in the pulmonary system if the GW9662 exposure time was increased. Thus, in future studies we may have to evaluate different exposure times of GW9662 to determine if similar developmental changes in NO signaling and ROS generation occurs with longer durations of PPAR-γ inhibition.

The other notable finding in this study is that PPAR-γ inhibition leads to an increase in mitochondrial-derived superoxide, correlating with the disruption of carnitine homeostasis. The carnitine transport system consists of CPT1 enzyme localized on the outer mitochondrial membrane and CPT2 enzyme on the inner mitochondrial membrane [38]. In addition, the final component of the carnitine shuttle is CrAT enzyme, which resides in the mitochondrial matrix and reconverts short- and medium chain acyl-CoAs into acyl carnitines using carnitine. This reversible acylation of carnitines modulates the intracellular concentrations of free CoA and acyl CoA [39]. Thus, decreases in either carnitine transport or CrAT activity will lead to an increase in acyl-CoA and the inhibition of oxidative metabolism [40–42]. This mitochondrial dysfunction associated with the decreased expression of CPT1, CPT2, and CrAT is similar to what we have previously observed in our lambs with increased PBF [12]. Further, our recent study in which we treated lambs with increased PBF with rosiglitazone demonstrated that stimulating PPAR-γ signaling preserved both carnitine homeostasis and NO signaling by maintaining mitochondrial function [43]. The regulation of the carnitine shuttle enzymes by PPAR-γ is complex. Only the CPT1 gene has been shown to possess a PPAR response element (PPRE) in its promoter region [44]. While PPARγ gene silencing has been shown to reduce the levels of CPT1 and CPT2 protein in cultured endothelial cells although only CPT2 mRNA levels are decreased [43]. However, PPARs have both gene-binding dependent, termed transactivation, and gene-binding independent, termed transrepression, effects. Transactivation involves the formation of heterodimers with the retinoid X-receptor. Activation by PPAR ligands results in the binding of the heterodimer to peroxisome proliferator response elements, located in the promoter regions of PPAR-regulated genes. Transrepression involves the binding of PPARs to transcription factors, such as NF-κB, which then alters their binding to DNA promoter elements. PPARs can also bind and sequester various cofactors for transcription factors, and thus further alter gene expression. Importantly, the precise effects of PPARs vary greatly between cell types. Thus, it is likely that the loss of PPAR-γ signaling with GW9662 is not the same as that in lambs with increased PBF where the exposure of the vascular endothelium to increased shear stress likely exerts other effects on endothelial structure and function that may alter the binding partners for PPAR-γ is which will in turn alter the transactivation and/or transrepression of a number of genes which could include the genes regulating carnitine homeostasis.

In conclusion, our data indicate that the attenuation of PPAR-γ signaling is sufficient to produce pulmonary endothelial dysfunction in the neonatal lamb and that this is a complex process involving mitochondrial dysfunction, increased NO and superoxide generation, and the nitration-mediated inhibition of PKG-Iα. Thus, our data confirm the key role played by PPAR-γ signaling in the development of pulmonary hypertension. Finally, we speculate that preserving carnitine homeostasis perhaps by stimulating PPAR-γ signaling may prevent the progression of pulmonary hypertension.

Acknowledgments

This research was supported in part by grants HL60190 (SMB), HL67841 (SMB), R21HD057406 (SMB), HL61284 (JRF) all from the National Institutes of Health, and by a grant from the *Fondation Leducq* (SMB and JRF), an AHA Scientist Development Grant (11SDG7460024, to SS) and by a Seed Award (SS) from the Cardiovascular Discovery Institute of Georgia Health Sciences University. RR was supported in part by National Institutes of Health Training Grant, 5T32-HL-06699.

LITERATURE CITED

1. Rabinovitch M, Bothwell T, Hayakawa BN, Williams WG, Trusler GA, Rowe RD, et al. Pulmonary artery endothelial abnormalities in patients with congenital heart defects and pulmonary

hypertension. A correlation of light with scanning electron microscopy and transmission electron microscopy. Lab Invest. 1986; 55:632–53. [PubMed: 3784535]

2. Celermajer DS, Cullen S, Deanfield JE. Impairment of endothelium-dependent pulmonary artery relaxation in children with congenital heart disease and abnormal pulmonary hemodynamics. Circulation. 1993; 87:440–6. [PubMed: 8425291]
3. Yoshibayashi M, Nishioka K, Nakao K, Saito Y, Matsumura M, Ueda T, et al. Plasma endothelin concentrations in patients with pulmonary hypertension associated with congenital heart defects. Evidence for increased production of endothelin in pulmonary circulation. Circulation. 1991; 84:2280–5. [PubMed: 1959183]
4. Tian J, Smith A, Nechtman J, Podolsky R, Aggarwal S, Snead C, et al. Effect of PPARgamma inhibition on pulmonary endothelial cell gene expression: gene profiling in pulmonary hypertension. Physiol Genomics. 2009; 40:48–60. [PubMed: 19825830]
5. Nisbet RE, Sutliff RL, Hart CM. The role of peroxisome proliferator-activated receptors in pulmonary vascular disease. PPAR Res. 2007; 2007:18797. [PubMed: 17710111]
6. Kersten S, Desvergne B, Wahli W. Roles of PPARs in health and disease. Nature. 2000; 405:421–4. [PubMed: 10839530]
7. Vamecq J, Latruffe N. Medical significance of peroxisome proliferator-activated receptors. Lancet. 1999; 354:141–8. [PubMed: 10408502]
8. Nicol CJ, Adachi M, Akiyama TE, Gonzalez FJ. PPARgamma in endothelial cells influences high fat diet-induced hypertension. Am J Hypertens. 2005; 18:549–56. [PubMed: 15831367]
9. Guignabert C, Alvira CM, Alastalo TP, Sawada H, Hansmann G, Zhao M, et al. Tie2-mediated loss of peroxisome proliferator-activated receptor-gamma in mice causes PDGF receptor-beta-dependent pulmonary arterial muscularization. Am J Physiol Lung Cell Mol Physiol. 2009; 297:L1082–90. [PubMed: 19801450]
10. Ameshima S, Golpon H, Cool CD, Chan D, Vandivier RW, Gardai SJ, et al. Peroxisome proliferator-activated receptor gamma (PPARgamma) expression is decreased in pulmonary hypertension and affects endothelial cell growth. Circ Res. 2003; 92:1162–9. [PubMed: 12714563]
11. Sutliff RL, Kang BY, Hart CM. PPARgamma as a potential therapeutic target in pulmonary hypertension. Ther Adv Respir Dis. 4:143–60. [PubMed: 20530063]
12. Sharma S, Sud N, Wiseman DA, Carter AL, Kumar S, Hou Y, et al. Altered carnitine homeostasis is associated with decreased mitochondrial function and altered nitric oxide signaling in lambs with pulmonary hypertension. Am J Physiol Lung Cell Mol Physiol. 2008; 294:L46–56. [PubMed: 18024721]
13. Aggarwal S, Gross CM, Kumar S, Datar S, Oishi P, Kalka G, et al. Attenuated vasodilatation in lambs with endogenous and exogenous activation of cGMP signaling: Role of protein kinase G nitration. J Cell Physiol. 2011
14. Tian J, Smith A, Nechtman J, Podolsky R, Aggarwal S, Snead C, et al. Effect of PPARgamma inhibition on pulmonary endothelial cell gene expression: gene profiling in pulmonary hypertension. Physiol Genomics. 2009; 40:48–60. [PubMed: 19825830]
15. Black SM, Fineman JR, Steinhorn RH, Bristow J, Soifer SJ. Increased endothelial NOS in lambs with increased pulmonary blood flow and pulmonary hypertension. Am J Physiol. 1998; 275:H1643–51. [PubMed: 9815072]
16. Reddy VM, Wong J, Liddicoat JR, Johengen M, Chang R, Fineman JR. Altered endothelium-dependent responses in lambs with pulmonary hypertension and increased pulmonary blood flow. Am J Physiol. 1996; 271:H562–70. [PubMed: 8770097]
17. Denninger JW, Marletta MA. Guanylate cyclase and the .NO/cGMP signaling pathway. Biochim Biophys Acta. 1999; 1411:334–50. [PubMed: 10320667]
18. Evora PR, Evora PM, Celotto AC, Rodrigues AJ, Joviliano EE. Cardiovascular Therapeutics Targets on the NO-sGC-cGMP Signaling Pathway: A Critical Overview. Curr Drug Targets. 2012; 13:1207–14. [PubMed: 22716077]
19. Sud N, Sharma S, Wiseman DA, Harmon C, Kumar S, Venema RC, et al. Nitric oxide and superoxide generation from endothelial NOS: modulation by HSP90. Am J Physiol Lung Cell Mol Physiol. 2007; 293:L1444–53. [PubMed: 17827253]

20. Chawla A, Repa JJ, Evans RM, Mangelsdorf DJ. Nuclear receptors and lipid physiology: opening the X-files. Science. 2001; 294:1866–70. [PubMed: 11729302]
21. Blanquart C, Barbier O, Fruchart JC, Staels B, Glineur C. Peroxisome proliferator-activated receptors: regulation of transcriptional activities and roles in inflammation. J Steroid Biochem Mol Biol. 2003; 85:267–73. [PubMed: 12943712]
22. Denning GM, Stoll LL. Peroxisome Proliferator-Activated Receptors: Potential Therapeutic Targets in Lung Disease? Pediatr Pulmonol. 2005
23. Oishi P, Sharma S, Datar S, Kumar S, Raff G, Azakie A, et al. Rosiglitazone preserves pulmonary vascular function in lambs with increased pulmonary blood flow. Pediatr Res. 2012 In Press.
24. Lu X, Murphy TC, Nanes MS, Hart CM. PPAR{gamma} regulates hypoxia-induced Nox4 expression in human pulmonary artery smooth muscle cells through NF-{kappa}B. Am J Physiol Lung Cell Mol Physiol.
25. Nisbet RE, Bland JM, Kleinhenz DJ, Mitchell PO, Walp ER, Sutliff RL, et al. Rosiglitazone attenuates chronic hypoxia-induced pulmonary hypertension in a mouse model. Am J Respir Cell Mol Biol. 42:482–90. [PubMed: 19520921]
26. Hansmann G, de Jesus Perez VA, Alastalo TP, Alvira CM, Guignabert C, Bekker JM, et al. An antiproliferative BMP-2/PPARgamma/apoE axis in human and murine SMCs and its role in pulmonary hypertension. J Clin Invest. 2008; 118:1846–57. [PubMed: 18382765]
27. Aggarwal S, Rafikov R, Gross CM, Kumar S, Pardo D, Black SM. Purification and functional analysis of protein kinase G-1alpha using a bacterial expression system. Protein Expr Purif. 2011
28. Burgoyne JR, Madhani M, Cuello F, Charles RL, Brennan JP, Schroder E, et al. Cysteine redox sensor in PKGIa enables oxidant-induced activation. Science. 2007; 317:1393–7. [PubMed: 17717153]
29. Zhao YY, Zhao YD, Mirza MK, Huang JH, Potula HH, Vogel SM, et al. Persistent eNOS activation secondary to caveolin-1 deficiency induces pulmonary hypertension in mice and humans through PKG nitration. The Journal of clinical investigation. 2009; 119:2009–18. [PubMed: 19487814]
30. Oishi P, Sharma S, Grobe A, Azakie A, Harmon C, Johengen MJ, et al. Alterations in cGMP, soluble guanylate cyclase, phosphodiesterase 5, and B-type natriuretic peptide induced by chronic increased pulmonary blood flow in lambs. Pediatr Pulmonol. 2007; 42:1057–71. [PubMed: 17902145]
31. Black SM, Sanchez LS, Mata-Greenwood E, Bekker JM, Steinhorn RH, Fineman JR. sGC and PDE5 are elevated in lambs with increased pulmonary blood flow and pulmonary hypertension. Am J Physiol Lung Cell Mol Physiol. 2001; 281:L1051–7. [PubMed: 11597895]
32. Grobe AC, Wells SM, Benavidez E, Oishi P, Azakie A, Fineman JR, et al. Increased oxidative stress in lambs with increased pulmonary blood flow and pulmonary hypertension: role of NADPH oxidase and endothelial NO synthase. Am J Physiol Lung Cell Mol Physiol. 2006; 290:L1069–77. [PubMed: 16684951]
33. Sharma S, Kumar S, Wiseman DA, Kallarackal S, Ponnala S, Elgaish M, et al. Perinatal changes in superoxide generation in the ovine lung: Alterations associated with increased pulmonary blood flow. Vascul Pharmacol. 2010; 53:38–52. [PubMed: 20362073]
34. Tian J, Fratz S, Hou Y, Lu Q, Gorlach A, Hess J, et al. Delineating the angiogenic gene expression profile before pulmonary vascular remodeling in a lamb model of congenital heart disease. Physiol Genomics. 2011; 43:87–98. [PubMed: 20978110]
35. Ovadia B, Reinhartz O, Fitzgerald R, Bekker JM, Johengen MJ, Azakie A, et al. Alterations in ET-1, not nitric oxide, in 1-week-old lambs with increased pulmonary blood flow. Am J Physiol Heart Circ Physiol. 2003; 284:H480–90. [PubMed: 12399254]
36. Oishi PE, Wiseman DA, Sharma S, Kumar S, Hou Y, Datar SA, et al. Progressive dysfunction of nitric oxide synthase in a lamb model of chronically increased pulmonary blood flow: a role for oxidative stress. Am J Physiol Lung Cell Mol Physiol. 2008; 295:L756–66. [PubMed: 18757524]
37. Xu H, Shi Y, Wang J, Jones D, Weilrauch D, Ying R, et al. A heat shock protein 90 binding domain in endothelial nitric-oxide synthase influences enzyme function. J Biol Chem. 2007; 282:37567–74. [PubMed: 17971446]

38. Kerner J, Hoppel C. Fatty acid import into mitochondria. Biochim Biophys Acta. 2000; 1486:1–17. [PubMed: 10856709]

39. Vaz FM, Wanders RJ. Carnitine biosynthesis in mammals. Biochem J. 2002; 361:417–29. [PubMed: 11802770]

40. Liu J, Atamna H, Kuratsune H, Ames BN. Delaying brain mitochondrial decay and aging with mitochondrial antioxidants and metabolites. Ann N Y Acad Sci. 2002; 959:133–66. [PubMed: 11976193]

41. Liu J, Head E, Gharib AM, Yuan W, Ingersoll RT, Hagen TM, et al. Memory loss in old rats is associated with brain mitochondrial decay and RNA/DNA oxidation: partial reversal by feeding acetyl-L-carnitine and/or R-alpha-lipoic acid. Proc Natl Acad Sci U S A. 2002; 99:2356–61. [PubMed: 11854529]

42. Liu J, Killilea DW, Ames BN. Age-associated mitochondrial oxidative decay: improvement of carnitine acetyltransferase substrate-binding affinity and activity in brain by feeding old rats acetyl-L- carnitine and/or R-alpha-lipoic acid. Proc Natl Acad Sci U S A. 2002; 99:1876–81. [PubMed: 11854488]

43. Sharma S, Sun X, Rafikov R, Kumar S, Hou Y, Oishi P, et al. PPAR-g regulates carnitine homeostasis and mitochondrial function in a lamb model of increased pulmonary blood flow. Plos One. 2012 In Press.

44. Mascaro C, Acosta E, Ortiz JA, Marrero PF, Hegardt FG, Haro D. Control of human muscle-type carnitine palmitoyltransferase I gene transcription by peroxisome proliferator-activated receptor. J Biol Chem. 1998; 273:8560–3. [PubMed: 9535828]

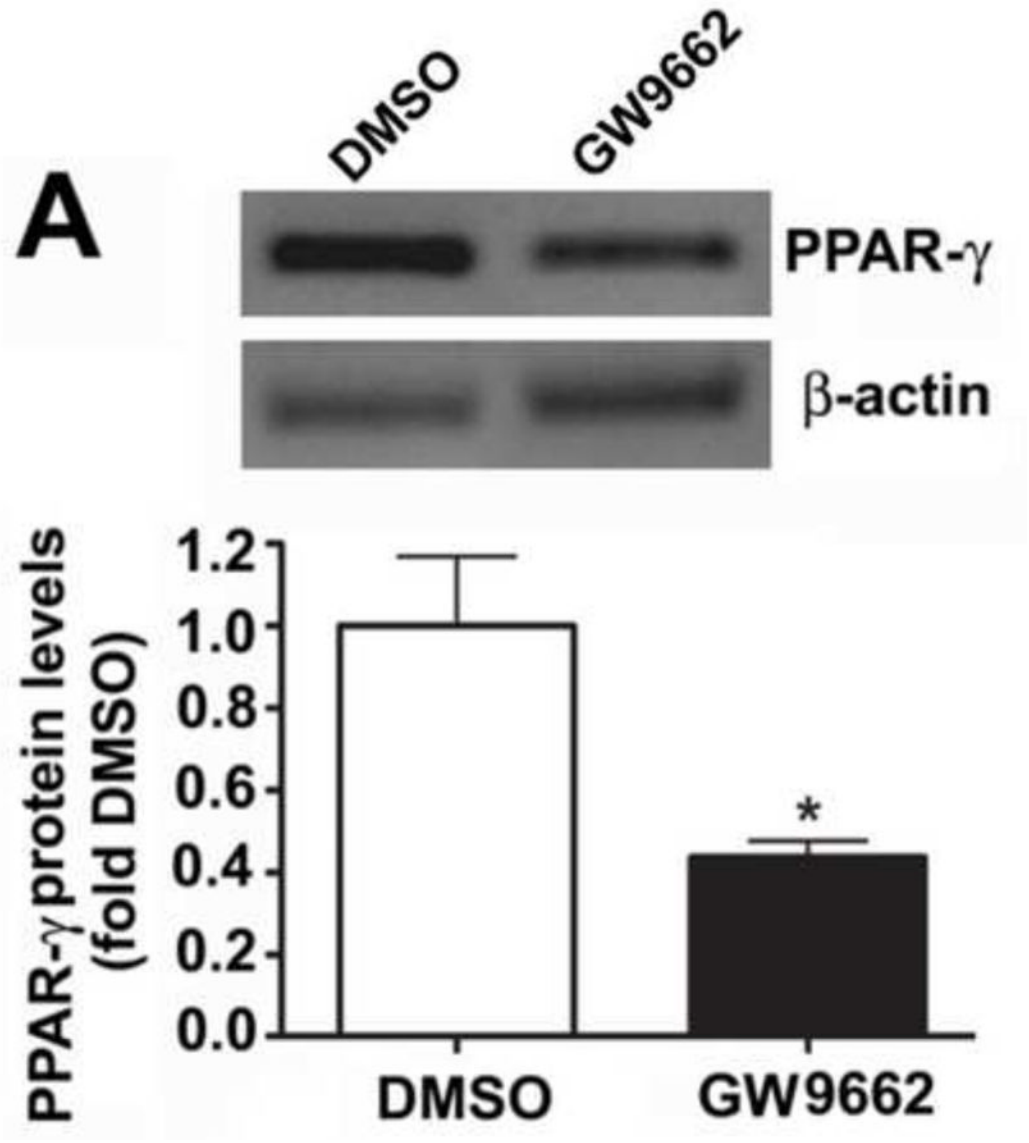

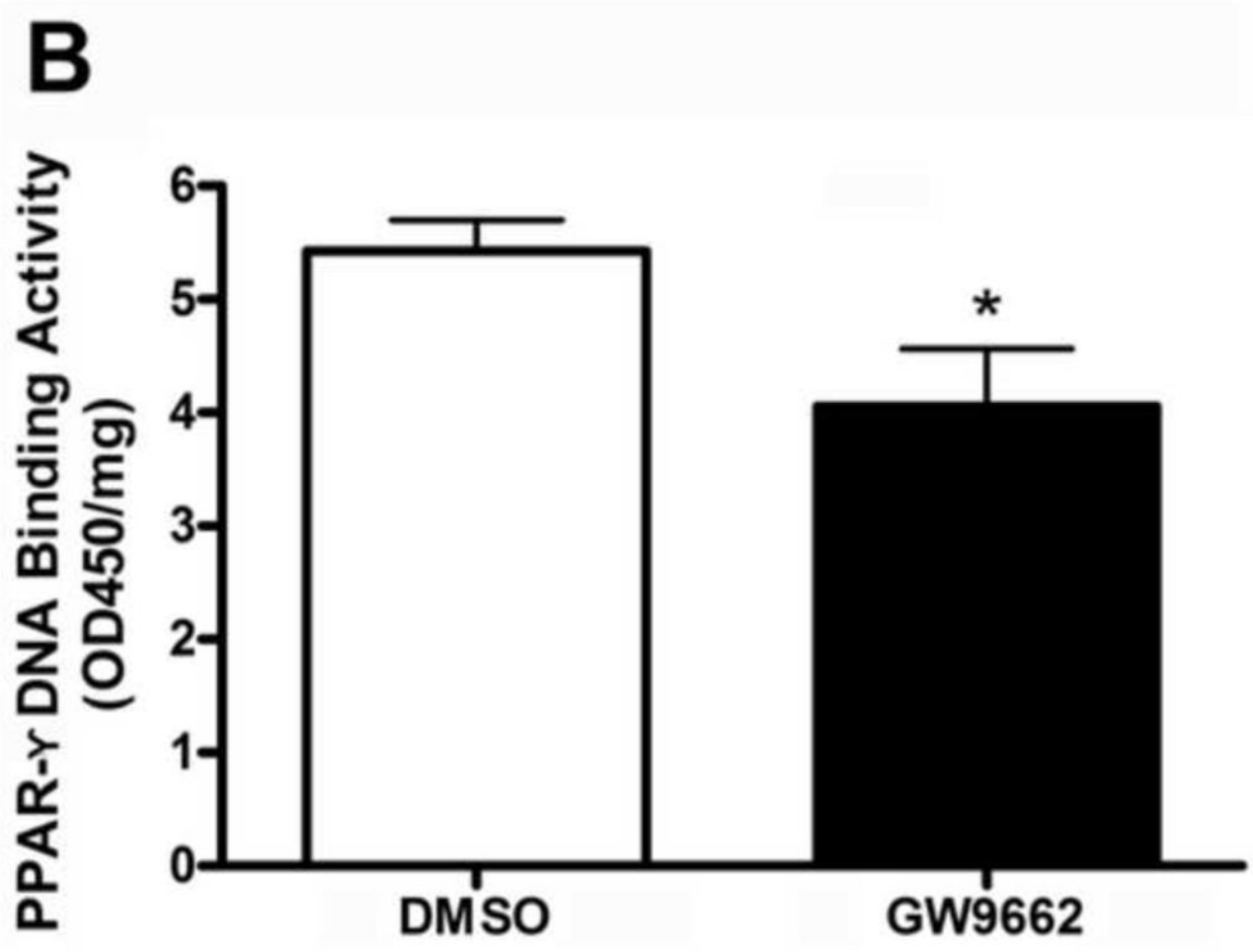

Figure 1. PPAR-γ inhibition decreases PPAR-γ protein levels and activity in the juvenile lamb lung

Protein extracts (30μg) prepared the peripheral lung of lambs exposed or not to the PPAR-γ antagonist, GW9662 (1mg/kg/day) for 2-weeks were analyzed by Western blot analysis and a significant decrease in both PPAR-γ protein levels (A) and PPAR-γ DNA-binding activity (B) was observed. Values are mean ± SE; n=5–6. *P <0.05 *vs*. DMSO control.

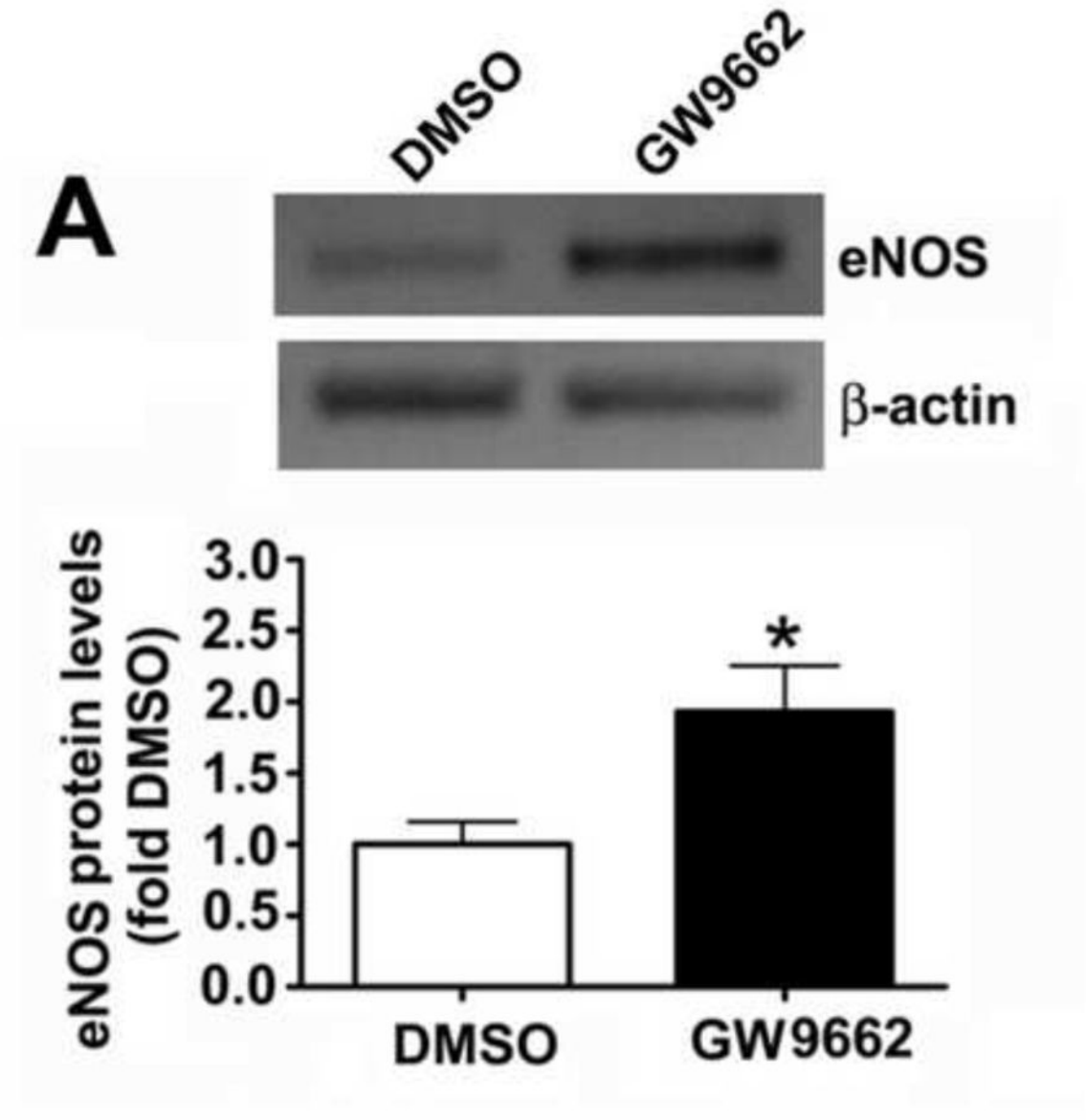

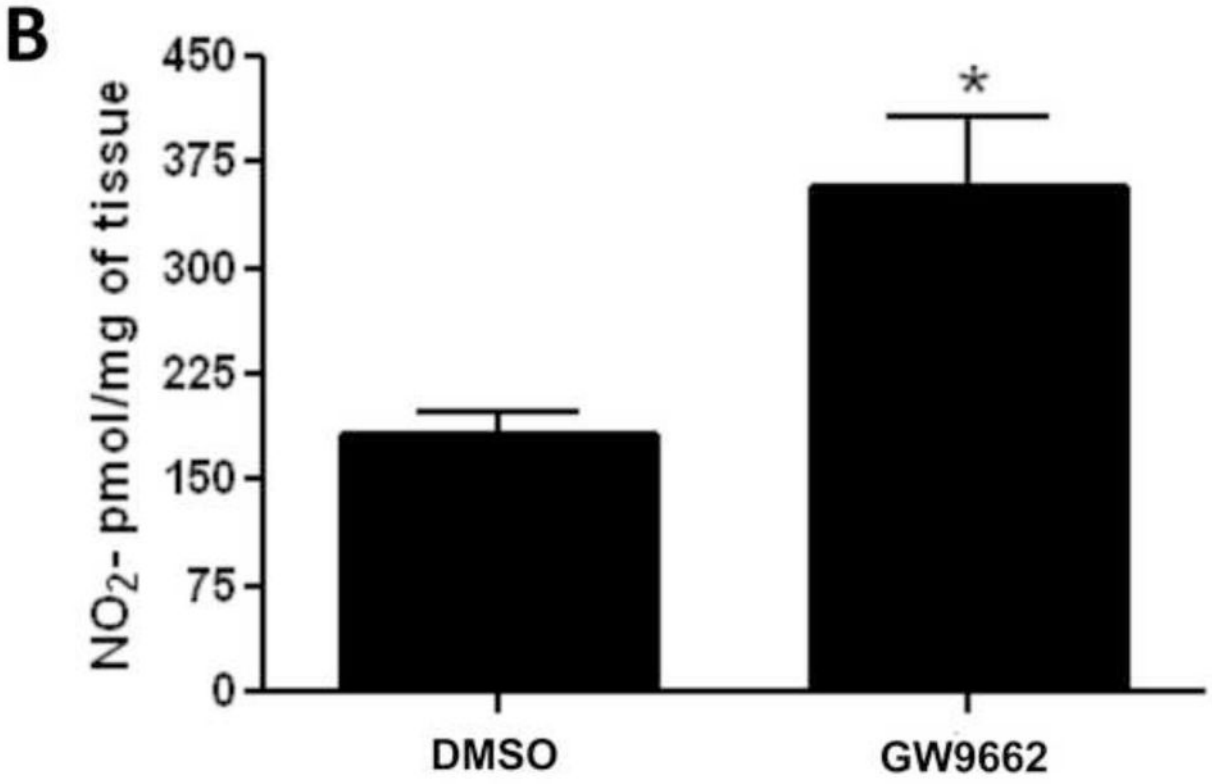

Figure 2. PPAR-γ inhibition increases NO signaling in the juvenile lamb lung

Protein extracts (30μg) prepared the peripheral lung of lambs exposed or not to the PPAR-γ antagonist, GW9662 (1mg/kg/day) for 2-weeks were analyzed by Western blot analysis and a significant increase in eNOS protein levels were observed (A). An increase in eNOS protein levels correlated with a significant increase in peripheral lung NO_x levels (B). Values are mean ± SE; n=5–6. *P <0.05 *vs.* DMSO control.

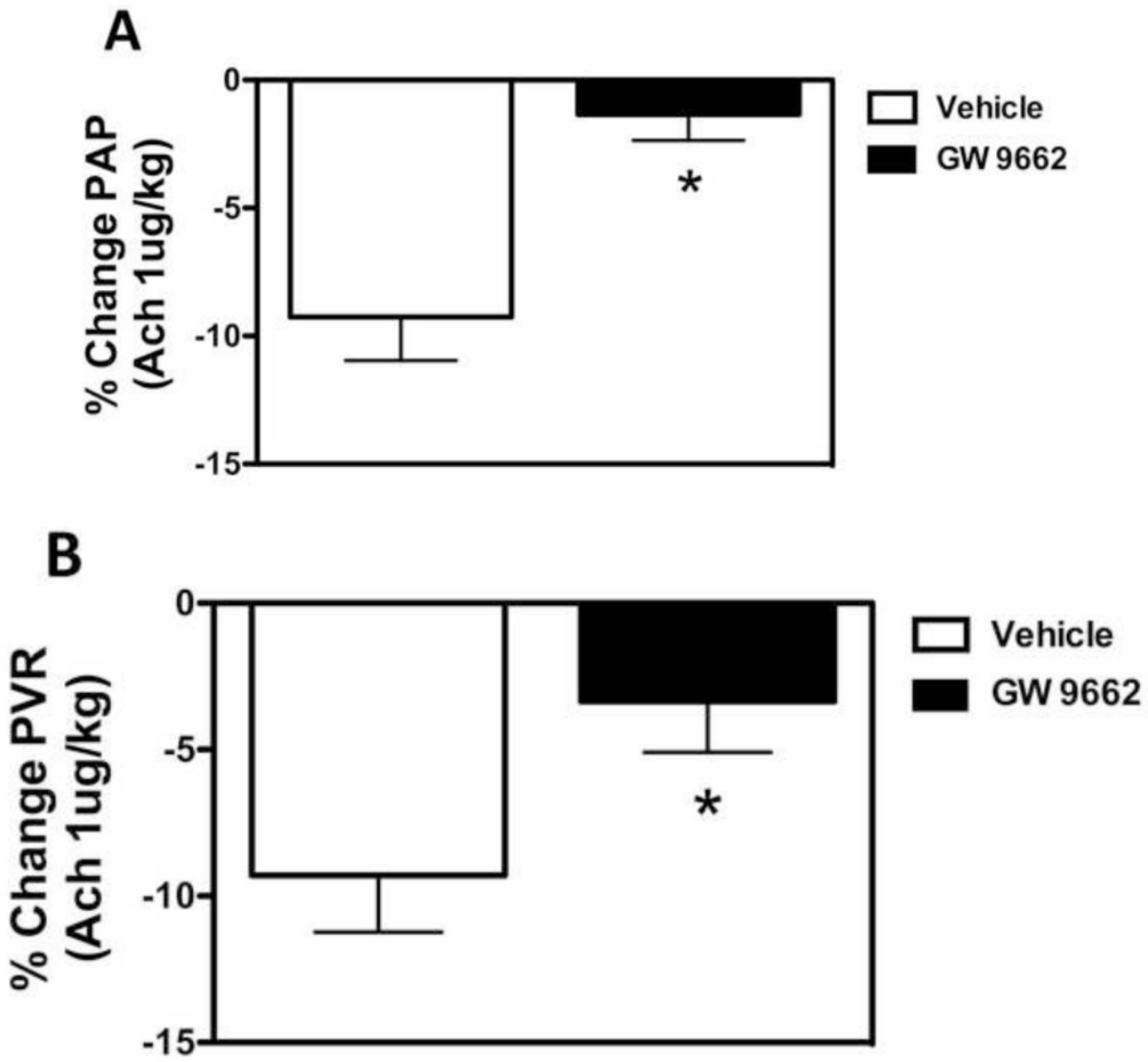

Figure 3. PPAR-γ inhibition induces pulmonary endothelial dysfunction in the juvenile lamb

Changes in main pulmonary arterial pressure (PAP), expressed as percent change from baseline, in response to acetylcholine (1 μg/kg), an endothelium-dependent agent in lambs exposed or not to the PPAR-γ antagonist, GW9662 (1mg/kg/day) for 2-weeks. Acetylcholine significantly decreased main pulmonary arterial pressure (A) and pulmonary vascular resistance (B) in DMSO-treated-, but not GW9662-treated lambs. Values are mean ± SD; n=5. *P<0.05 compared to baseline.

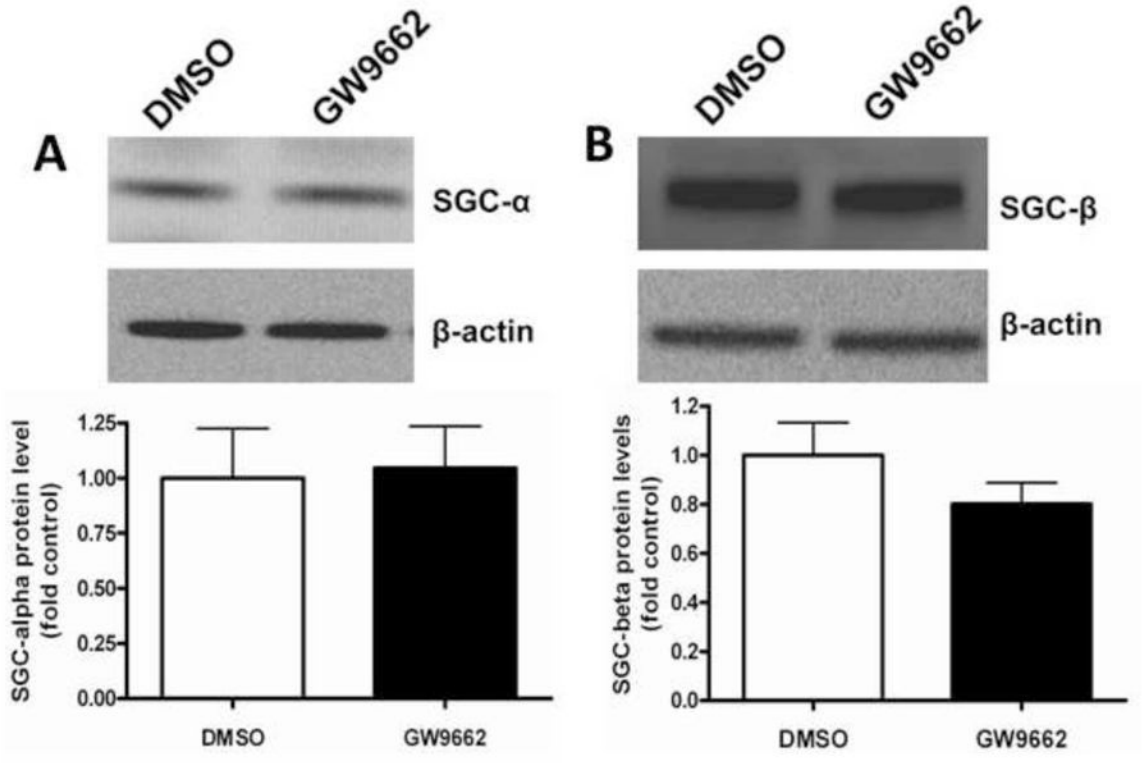

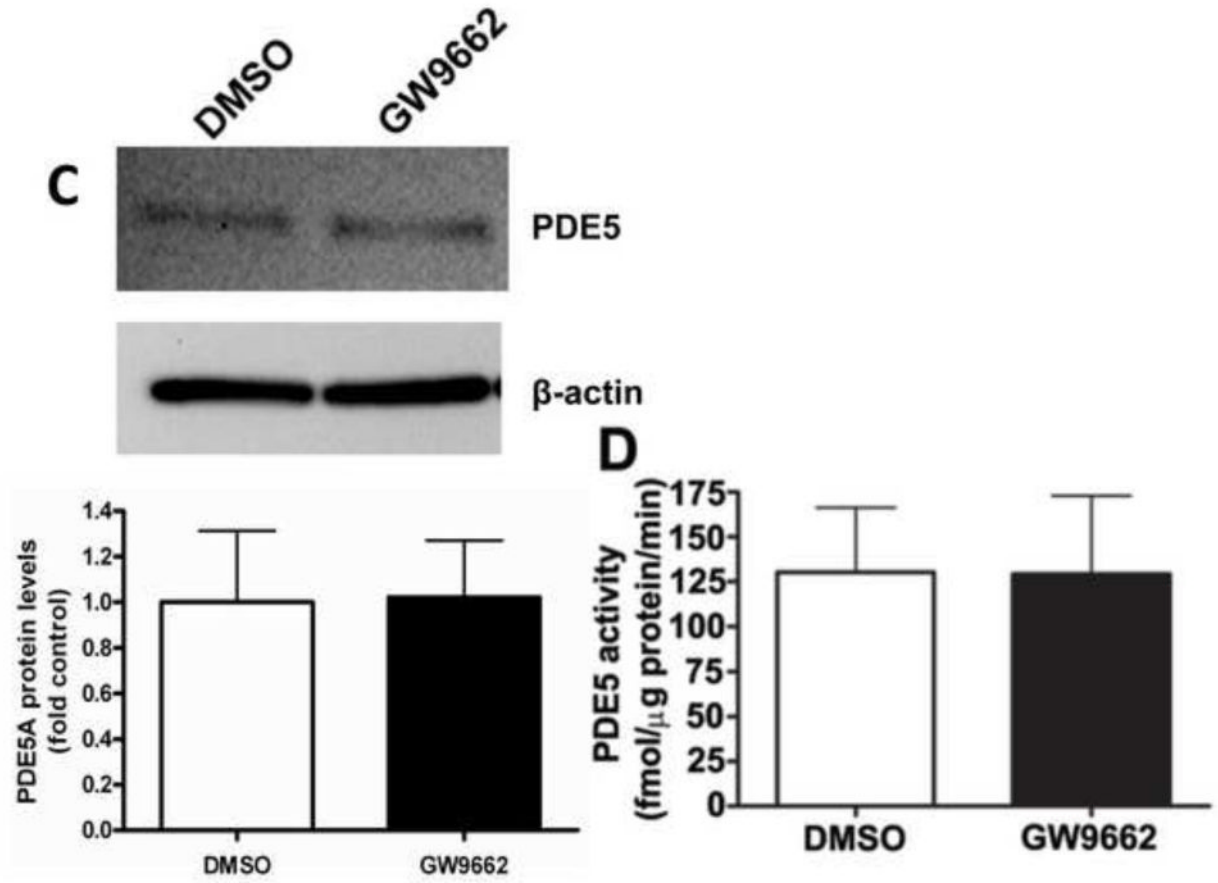

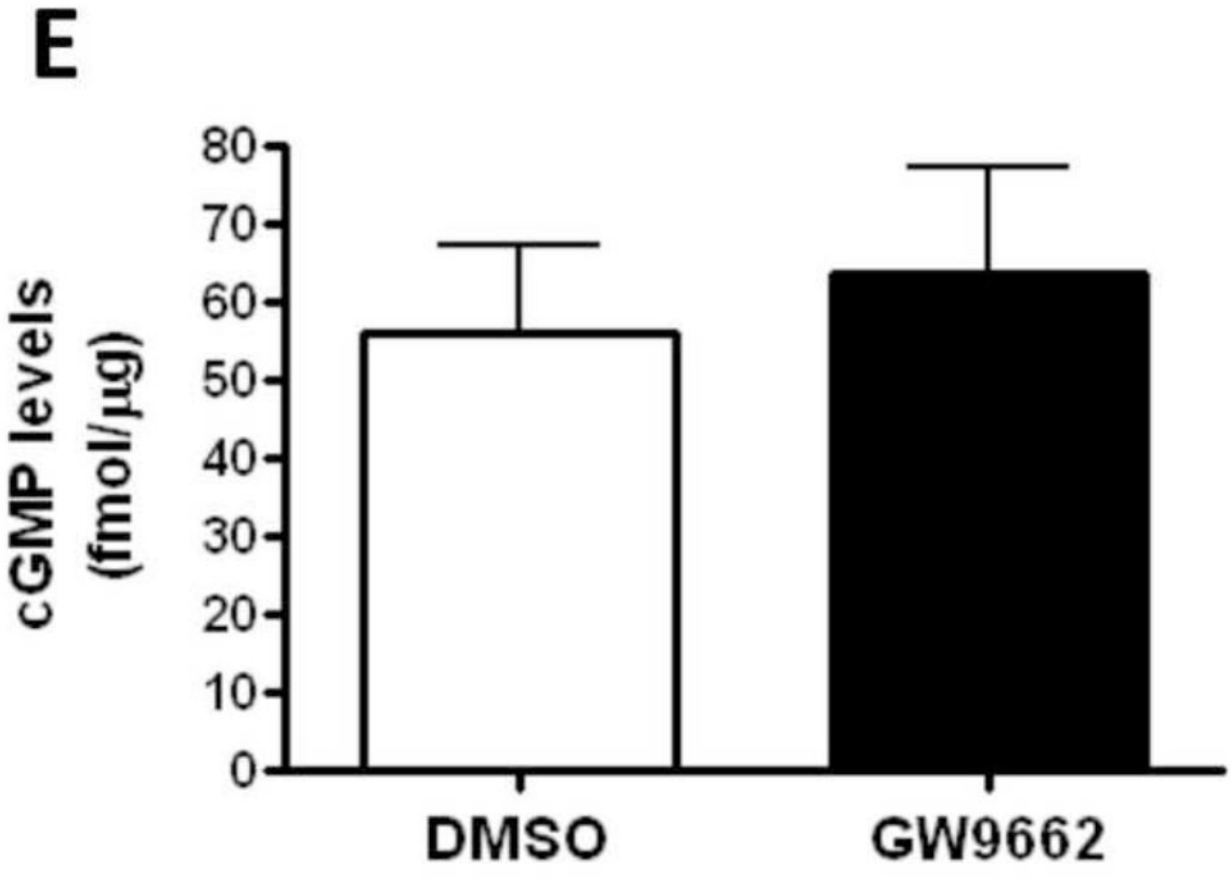

Figure 4. PPAR-γ inhibition does not alter cGMP levels in the juvenile lamb lung

Protein extracts (30μg) prepared the peripheral lung of lambs exposed or not to the PPAR-γ antagonist, GW9662 (1mg/kg/day) for 2-weeks were analyzed by Western blot analysis for changes in sGC-α1 (A), sGC-β1 (B) or PDE5 (C) protein levels. In addition, PDE5 activity (D) and cGMP levels (E) were determined. No significant differences were found between DMSO- and GW9662-treated lambs. Values are mean ± SE; n=5–6.

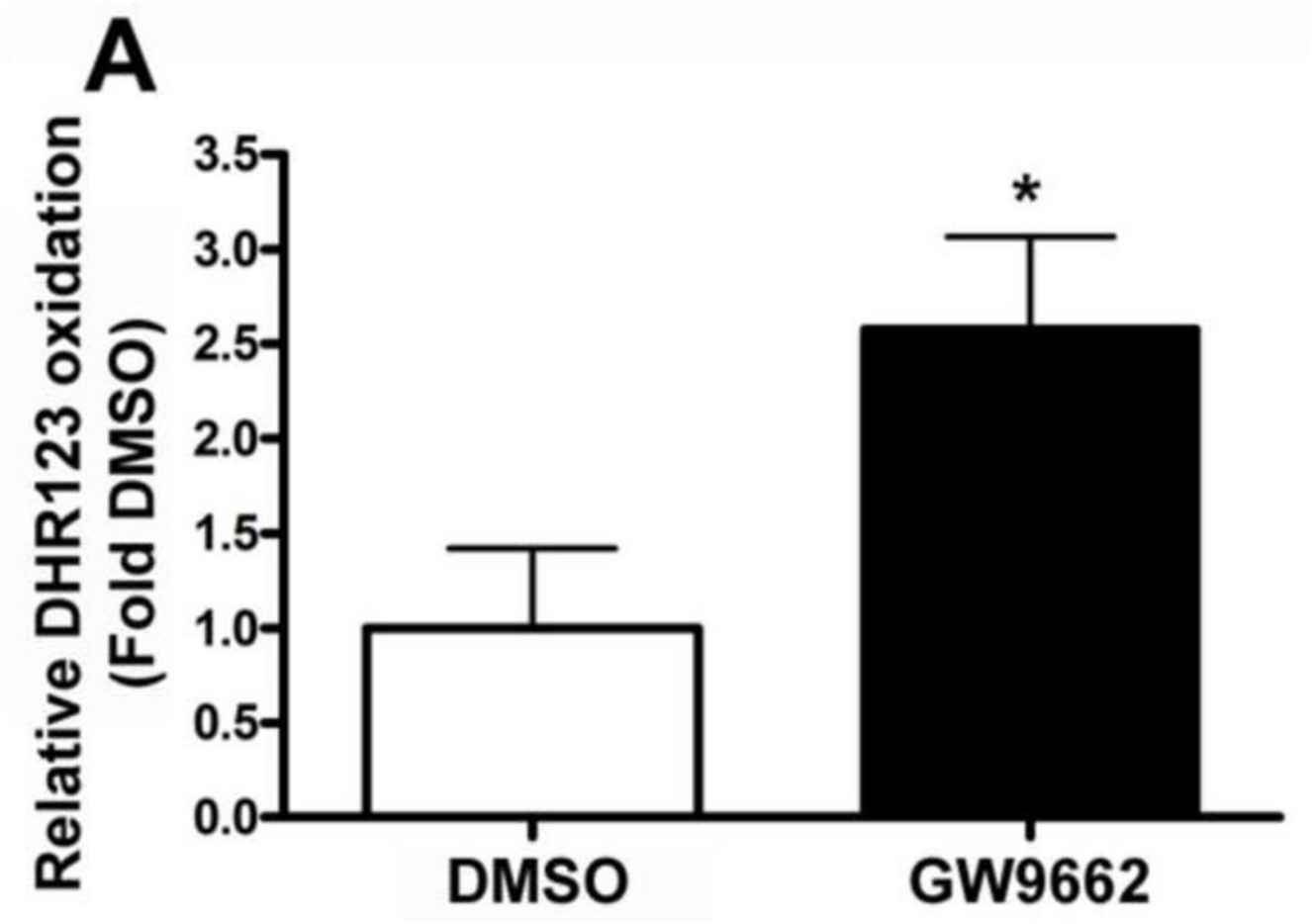

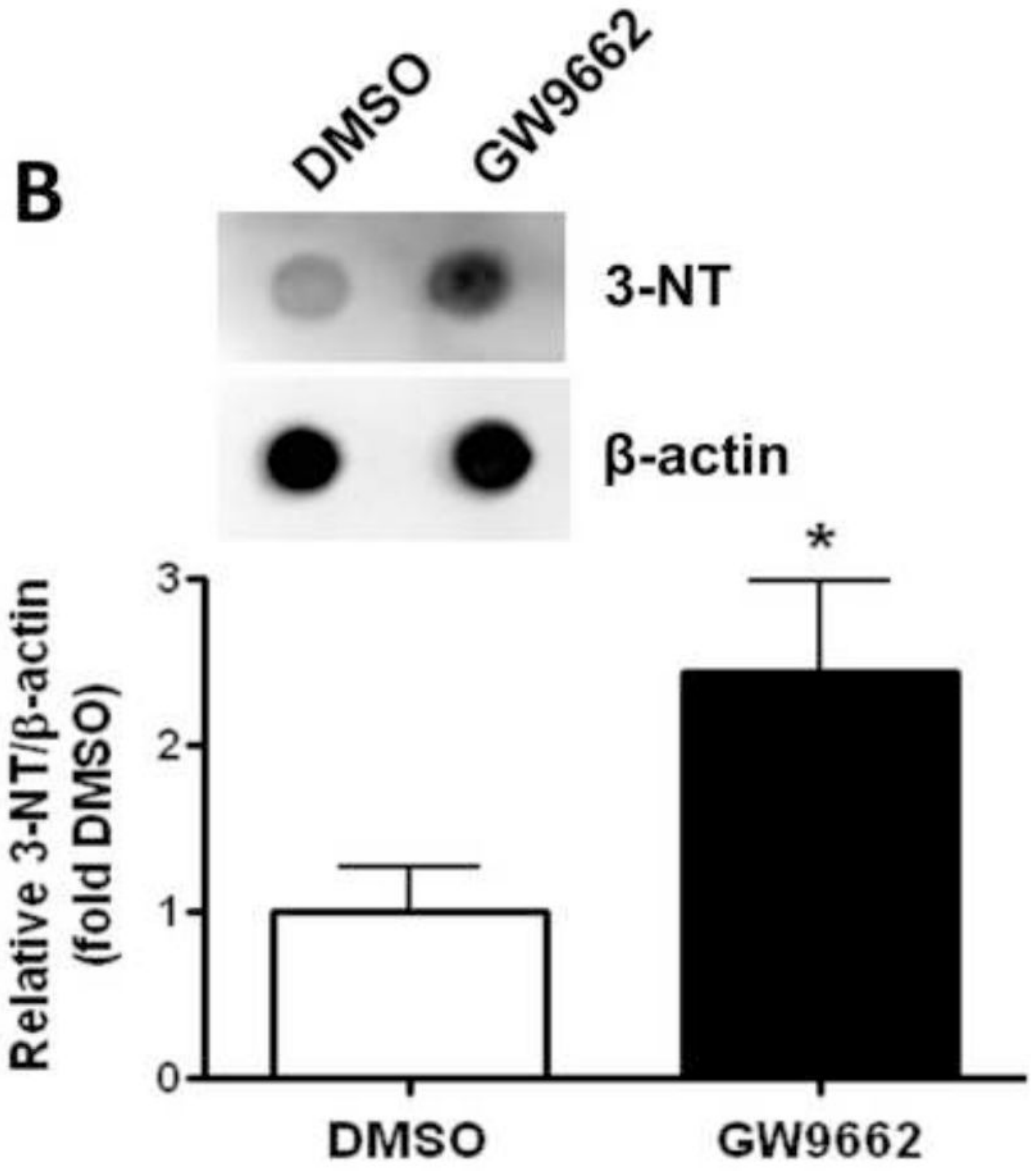

Figure 5. PPAR-γ inhibition increases peroxynitrite generation in the juvenile lamb lung

Peroxynitrite levels were determined by monitoring total nitrated protein using a dot-blot analysis (A) and by the oxidation of DHR 123 to rhodamine 123 (B) in the peripheral lung of lambs exposed or not to the PPAR-γ antagonist, GW9662 (1mg/kg/day) for 2-weeks. There is a significant increase in both total nitrated proteins (A) and DHR 123 oxidation (B) in the GW9662-treated lambs. Values are mean ± SE; n=5–6. *P <0.05 *vs.* DMSO control.

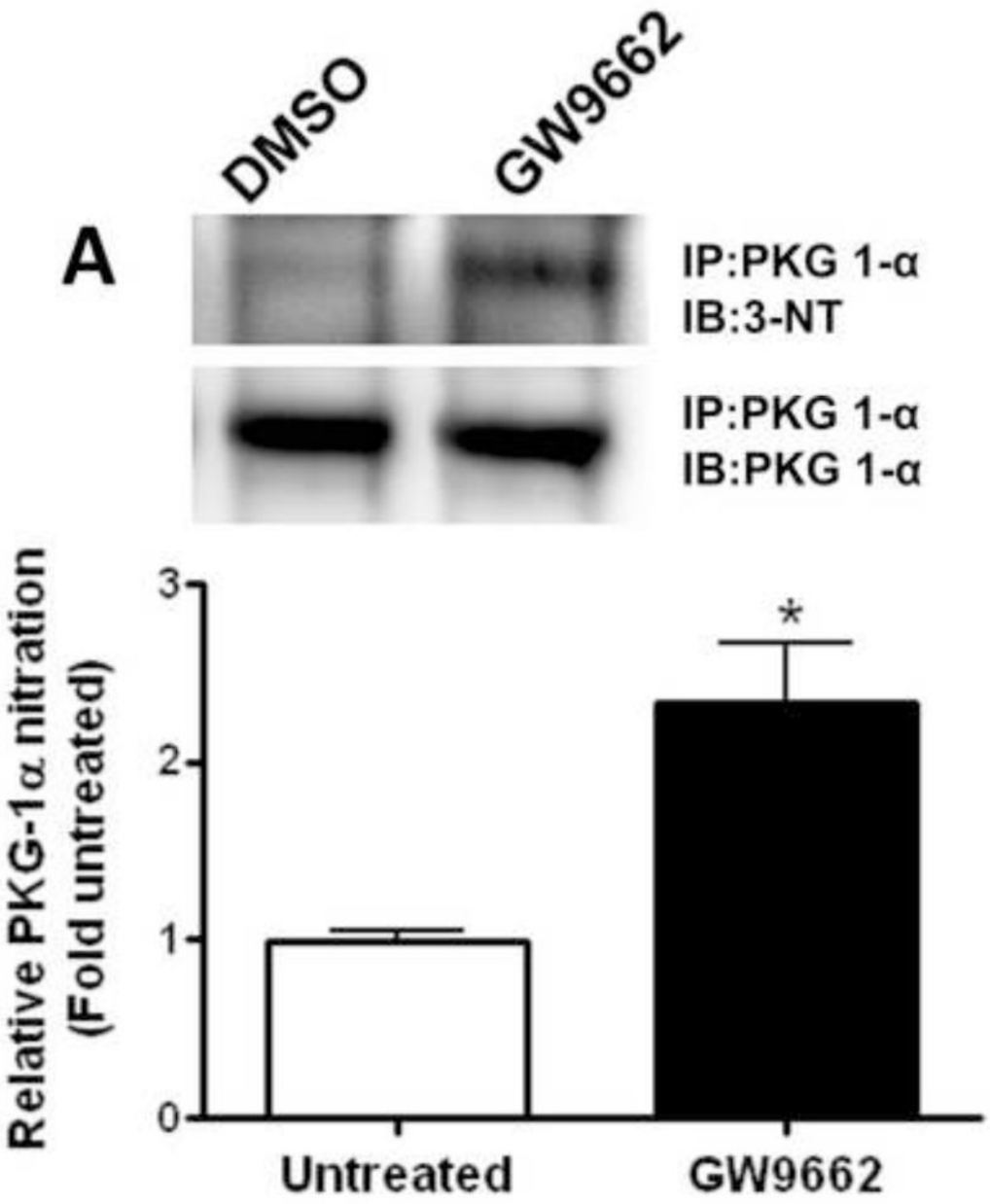

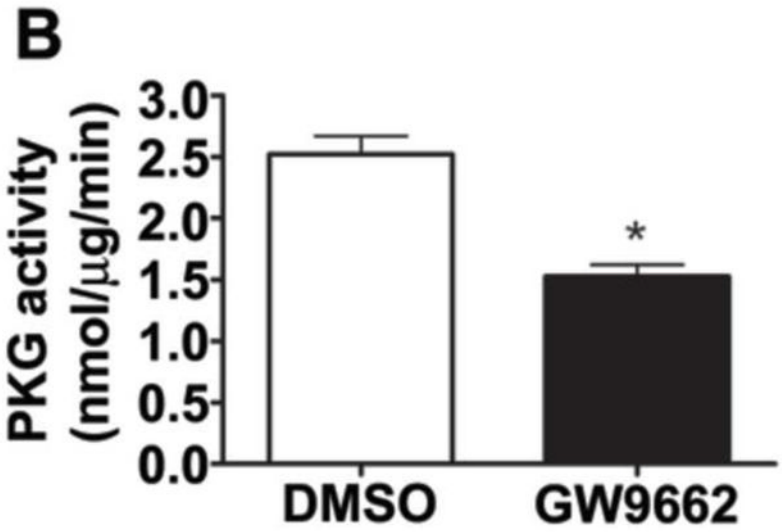

Figure 6. PPAR-γ inhibition increases PKG-1α nitration and decreases PKG activity in the juvenile lamb lung

Protein extracts (1000μg) prepared from the peripheral lung of lambs exposed or not to the PPAR-γ antagonist, GW9662 (1mg/kg/day) for 2-weeks were subjected to immunoprecipitation analysis using an antibody raised against PKG-1α. The level of nitrated PKG-1α was then determined using western blot analysis and an antiserum raised against 3-nitrotyrosine (A). Blots were then stripped and reprobed for PKG-1α to normalize for the efficiency of the immunoprecipitation. There is a significant increase in PKG-1α nitration in the GW9662-treated lambs (A). Using an ELISA based assay, we also found that total PKG activity is attenuated in GW9662-treated lambs (B). Values are mean ± SE; n=5–6. *P <0.05 *vs.* DMSO control.

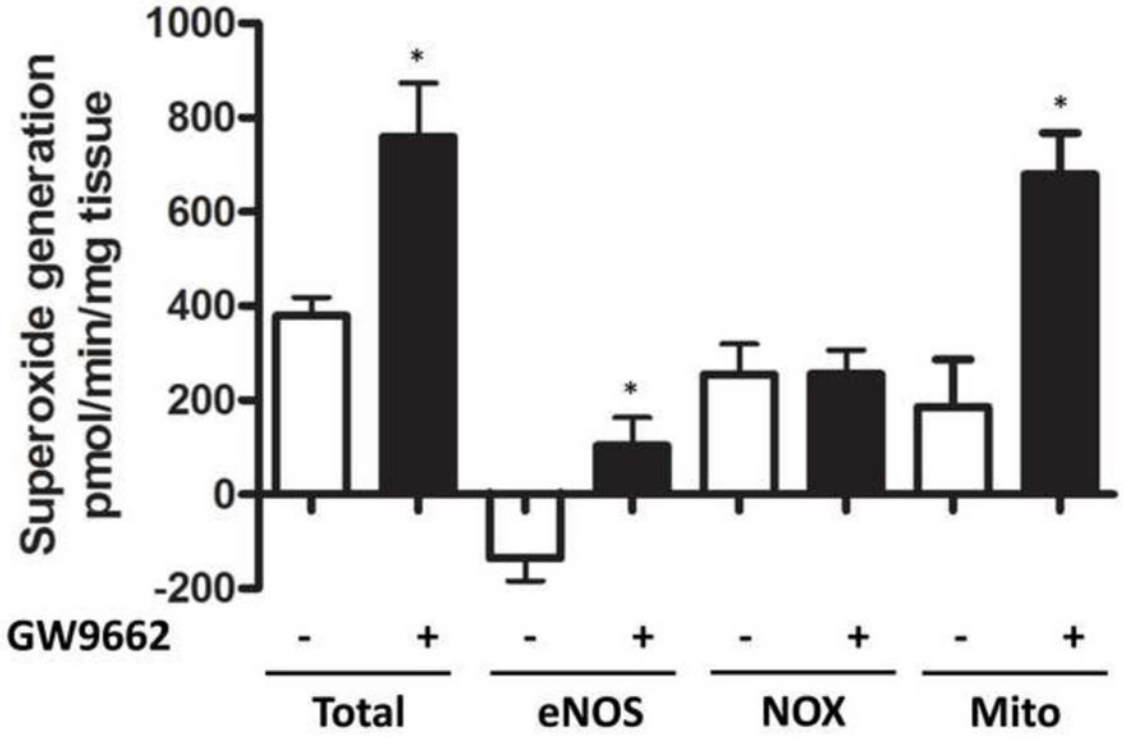

Figure 7. PPAR-γ inhibition increases mitochondrial derived superoxide in the juvenile lamb lung

Superoxide levels in the peripheral lung of lambs exposed or not to the PPAR-γ antagonist, GW9662 (1mg/kg/day) for 2-weeks were estimated by electron paramagnetic resonance (EPR) assay using 1-hydroxy-3-methoxycarbonyl-2,2,5,5-tetramethylpyrrolidine·HCl (CMH), which forms a stable chemical product with superoxide. There is a significant increase in total superoxide in the GW9662-treated lambs and this is mitochondrial derived. Values are mean ± SE; n=5–6. *P <0.05 *vs.* DMSO control.

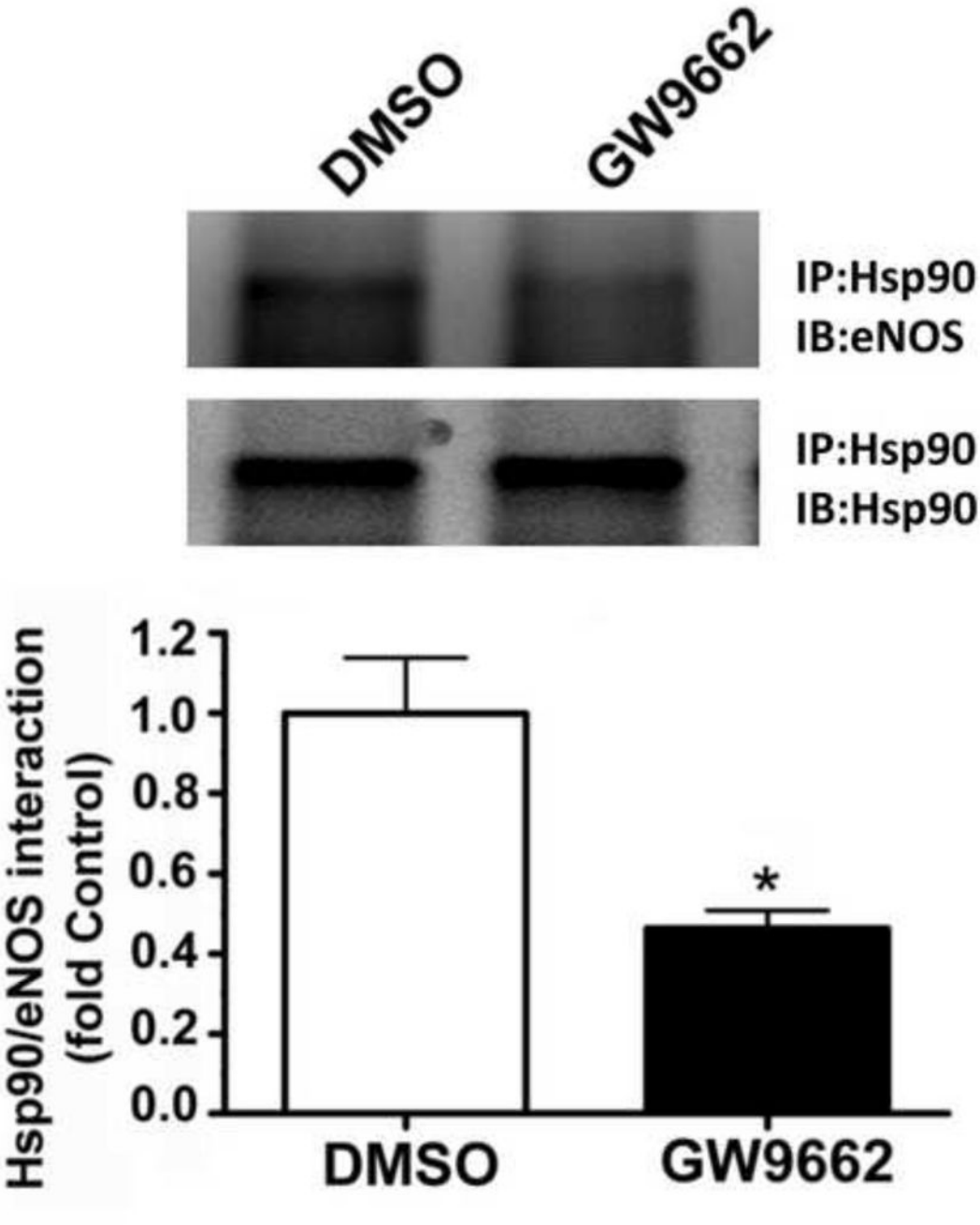

Figure 8. PPAR-γ inhibition decreases the interaction of eNOS with Hsp90 in the juvenile lamb lung

Protein extracts (1000μg) prepared from the peripheral lung of lambs exposed or not to the PPAR-γ antagonist, GW9662 (1mg/kg/day) for 2-weeks were subjected to immunoprecipitation analysis using an antibody raised against Hsp90. The level of eNOS interacting with Hsp90 was then determined using Western blot analysis and an antiserum raised against eNOS. Blots were then stripped and reprobed for Hsp90 to normalize for the efficiency of the immunoprecipitation. There is a significant decrease in the interaction of eNOS with Hsp90 in the GW9662-treated lambs. Values are mean ± SE; n=5–6. *P <0.05 *vs.* DMSO control.

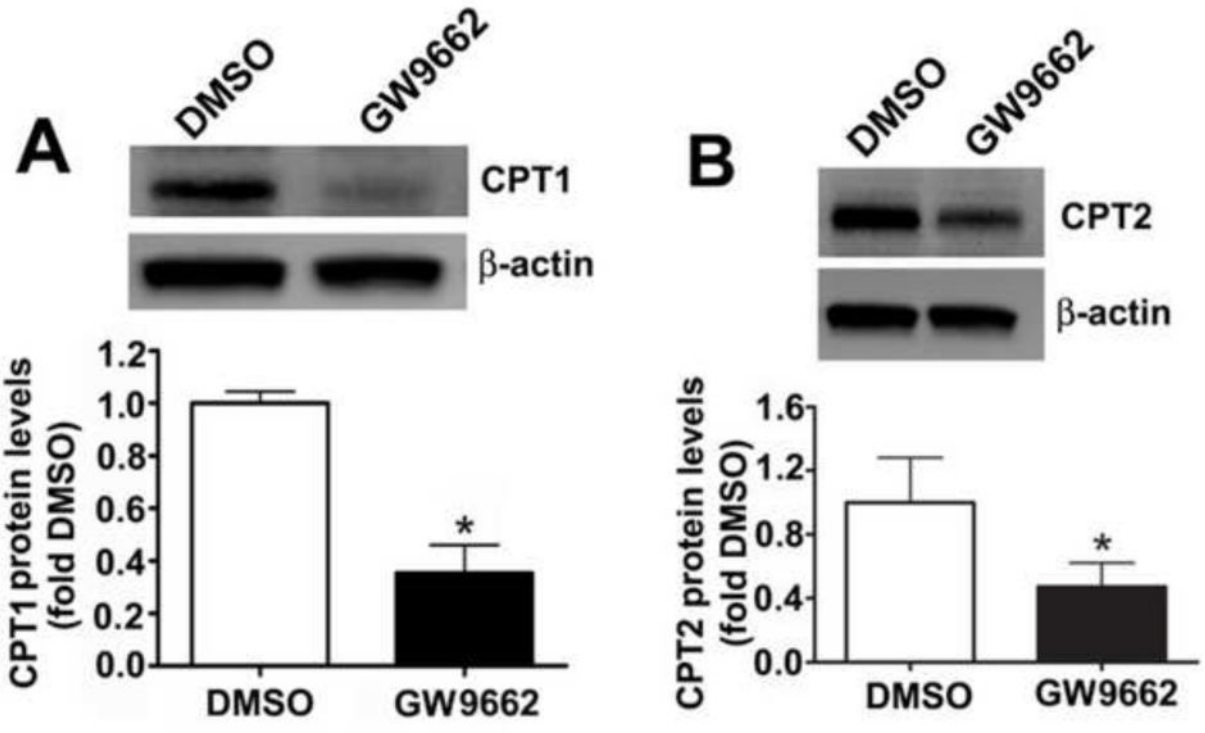

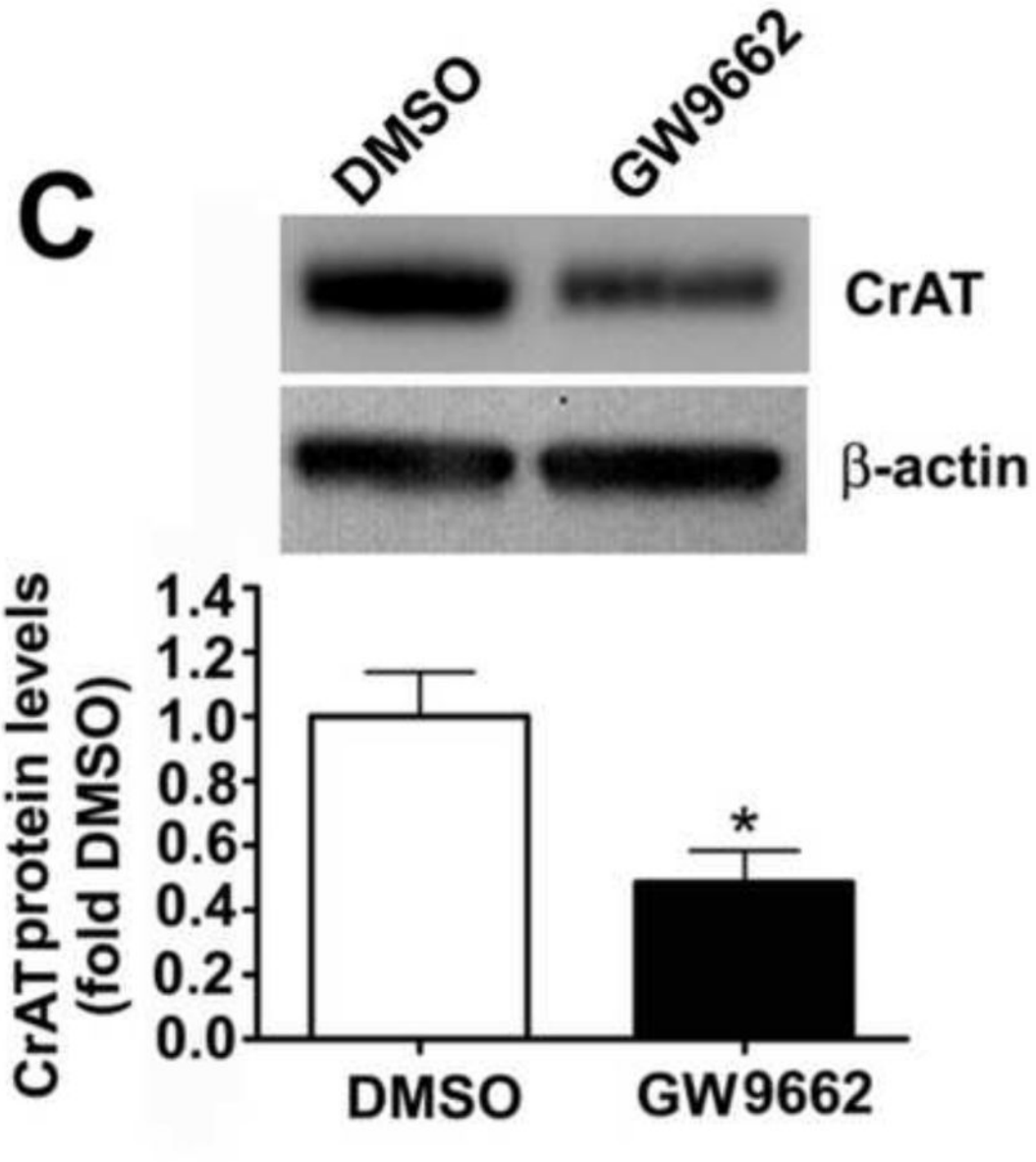

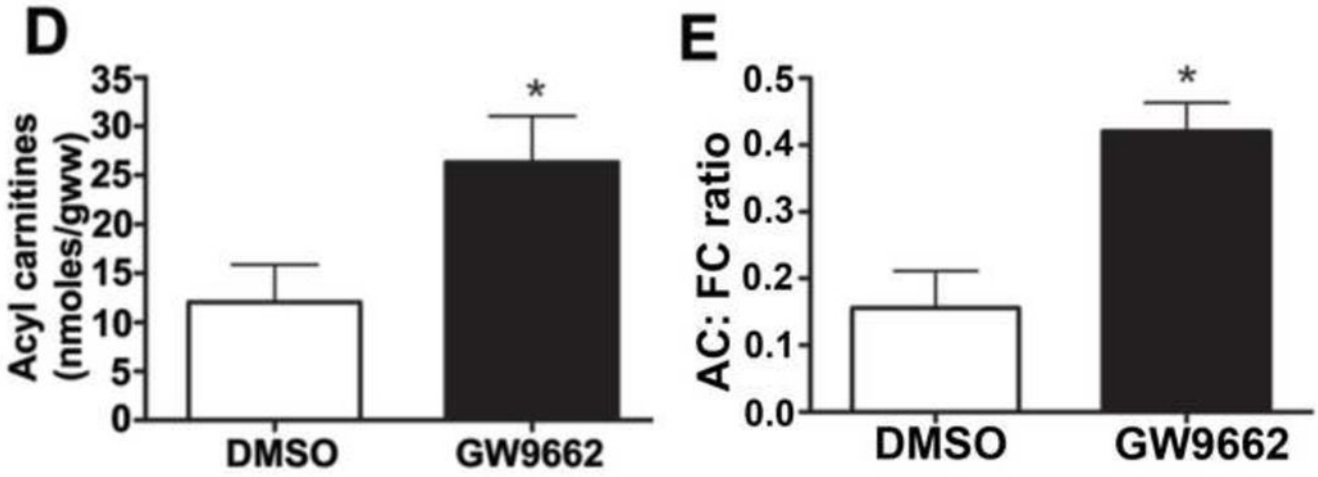

Figure 9. PPAR-γ inhibition disrupts carnitine homeostasis in the juvenile lamb lung

Protein extracts (30–50μg) were prepared the peripheral lung of lambs exposed or not to the PPAR-γ antagonist, GW9662 (1mg/kg/day) for 2-weeks were. CPT1 (A), CPT2 (B) and CrAT (C) protein levels were then determined by Western blot analyses. There was a significant decrease in all three proteins in the GW9662-treated lambs. Acyl carnitines (D) and the AC:FC ratio (E) were also found to be significantly higher in the GW9662-treated lambs, indicating disruption of carnitine homeostasis. Values are mean ± SE; n=5–6. *P <0.05 *vs.* DMSO control.

TABLE 1

GENERAL HEMODYNAMIC VARIABLES

Hemodynamic Variable	Vehicle (n=5)	GW9662 (n=5)
mPAP (mmHg)	14.2 ± 0.93	13.9 ± 1.3
mSAP (mmHg)	56.7 ± 3.2	62.7 ± 10.6
mRAP (mmHg)	2.6 ± 0.79	3.0 ± 0.77
mLAP (mmHg)	4.6 ± 0.74	3.9 ± 0.83
HR	149 ± 15	155 ± 21
Q_{lpa} (ml/min/kg)	67.3 ± 14.8	70.3 ± 27.4
PVR_{left} (mmHg/ml/min/kg)	0.15 ± 0.04	0.17 ± 0.08

mRAP: mean right atrial pressure, mPAP: mean pulmonary arterial pressure, mLAP: mean left atrial pressure, mSAP: mean systemic arterial pressure, Q_{lpa}: blood flow through the left pulmonary artery, PVR_{left}: left pulmonary vascular resistance. Values are mean ± S.D.